JOC The Journal of Organic Chemistry

Article

pubs.acs.org/joc

Base-Promoted Oxidative Cycloaddition Reaction of [60]Fullerene with Ethyl Acetoacetate for C_{60} Bis-2′,3′-dihydrofuran Derivatives: Effect of Bulky Addends

Si Chen,[†,‡] Zong-Jun Li,[†] and Xiang Gao*[,†]

[†]State Key Laboratory of Electroanalytical Chemistry, Changchun Institute of Applied Chemistry, University of Chinese Academy of Sciences, Chinese Academy of Sciences, 5625 Renmin Street, Changchun, Jilin 130022, China

[‡]College of Chemistry and Chemical Engineering, Yantai University, 30 Qingquan Road, Yantai, Shandong 264005, China

Supporting Information

ABSTRACT: The base-promoted oxidative cycloaddition reaction of [60]fullerene with ethyl acetoacetate was investigated. The reaction resulted in C_{60} bis-2′,3′-dihydrofuran derivatives, but only with the *trans*-1, *trans*-2, *trans*-3, and *e* configurations rather than any *cis* or *trans*-4 structures, demonstrating a new regioselectivity resulting from steric influence on C_{60} bisaddition. In addition, distribution of the bisadducts was complicated by the unsymmetrical nature of the addends, where each individual configuration may consist of several regioisomers.

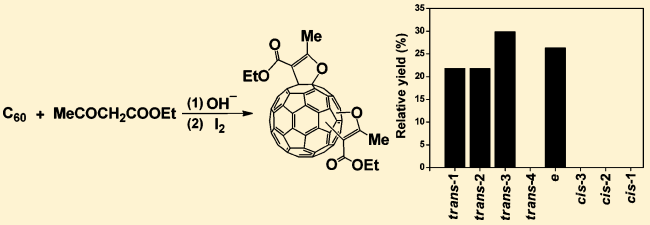

INTRODUCTION

Study of bisaddition of [60]fullerene is of importance in fullerene chemistry, because it not only reveals the intrinsic reactivity of [60]fullerene,[1,2] but also produces bisadducts that have a performance better than that of the monoadducts for construction of photovoltaic devices due to the increase of the LUMO level of the molecules caused by further cleavage of the π-conjugation of fullerenes.[3,4] Previous work has shown that bisadducts with the *cis*-1, *e*, and *trans*-3 configurations are typically preferred among all eight possible regioisomers when less sterically demanding addends are involved, due to the enhanced distribution of the frontier orbitals at these sites in the monoadducts, while only the formation of *cis*-1 regioisomer is inhibited when sterically demanding addends are used and the regioselectivity for other regioisomers remains essentially the same.[1,2] In principle, the formation of all *cis* adducts may be inhibited when the addends are extremely sterically demanding, and it would be intriguing to find out whether such a strong steric hindrance may enhance the production of the *trans* adducts as a trade-off. However, to the best of our knowledge, no such work has been carried out so far.

Base- or metal-promoted oxidative cycloaddition reactions of [60]fullerene with β-dicarbonyl compounds lead to the formation of 2′,3′-dihydrofuran C_{60} heterocycles.[5,6] However, only the monoheterocyclic C_{60} derivatives have been obtained, while no bis-2′,3′-dihydrofuran C_{60} derivative has been reported so far, similar to the cases of heterocycloaddition reactions of fullerenes involving the formation of a C_{60}–X (X = N or O) bond, where the bis-heterocyclic C_{60} adducts are rarely obtained.[7] Herein we report the base-promoted oxidative cycloaddition reaction of [60]fullerene with ethyl acetoacetate. Regioisomeric bis-2′,3′-dihydrofuran C_{60} derivatives **1** (Figure 1) are obtained for the first time. Interestingly, due to the bulky size of the addends, the formation of the *cis* adducts is completely inhibited, while the formation of the *trans* adducts is greatly enhanced. In addition, the structures of the products are complicated by the unsymmetrical nature of the addends.

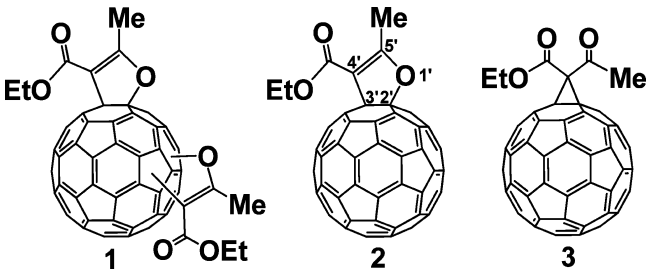

Figure 1. Regioisomeric bis-2′,3′-dihydrofuran C_{60} derivatives (**1**), mono-2′,3′-dihydrofuran C_{60} (**2**), and methanofullerene (**3**).

RESULTS AND DISCUSSION

Synthesis of Bis-2′,3′-dihydrofuran C_{60} Derivatives (1) and Preliminary Structural Assignment of the Bisadducts by HPLC Elution Order. Table 1 lists the screening of the reaction conditions. As shown in Table 1, both OH^- and I_2 are important for the reaction, where in addition to bis-2′,3′-dihydrofuran C_{60} derivatives (**1**), mono-2′,3′-dihydrofuran C_{60}

Received: October 15, 2015
Published: November 20, 2015

DOI: 10.1021/acs.joc.5b02392
J. Org. Chem. 2016, 81, 121−128

Table 1. Condition Screening for Preparing Bis-2′,3′-dihydrofuran C_{60} Derivatives

entry	OH^- (equiv)	I_2 (equiv)	temp (°C)	time[b] (min)	time[c] (min)	product (% yield)[d]
1	3	2	rt	30	5	**2**(26), **3**(32)
2	3	5	rt	30	5	**2**(23), **3**(33)
3	5	1.1	rt	30	5	**1**(6), **2**(9), mostly insoluble
4	5	2.2	rt	30	5	**1**(27), **2**(17),
5	5	6	rt	30	5	**2**(9), **3**(11), other bisadducts
6	10	11	rt	30	5	more polar products
7	5	2.2	80	30	5	mostly insoluble

[a]Reaction conditions: C_{60} (36 mg, 50 μmol) and ethyl acetoacetate (500 μL, 79 equiv) were put into *o*-DCB (*o*-dichlorobenzene) (15 mL). The mixture was stirred for 15 min under argon at the preset temperature. Then OH^- (TBAOH, tetra-*n*-butylammonium hydroxide, 1.0 M in CH_3OH) was added to the solution and the reaction was allowed to proceed for 30 min. The reaction was then quenched with I_2 for 5 min. [b]Time for reaction of C_{60} with OH^- and ethyl acetoacetate. [c]Time after I_2 was added into the mixture of C_{60}, OH^-, and ethyl acetoacetate. [d]Isolated yield.

(**2**),[6a] and methanofullerene (**3**)[6b] (Figure 1) were also produced during the screening. When a ratio of n_{OH-}:n_{C60} = 3:1 was used (entries 1 and 2), compounds **2** and **3** were obtained as the major products, while variation of I_2 from 2 to 5 equiv with respect to C_{60} had little effect on the product distribution. Further increase of OH^- to 5 equiv with respect to C_{60} and the use of 1.1 or 2.2 equiv of I_2 with respect to C_{60} (entries 3 and 4) resulted in bis-2′,3′-dihydrofuran C_{60} derivatives (**1**) and **2**. However, the use of less I_2 (entry 3) produced much more insoluble material than the case of using more I_2 (entry 4), likely due to polymerization involving C_{60} epoxide species[8] caused by the aerobic oxidation of anionic C_{60} species during the following workup (exposure to air),[9] indicating that the formation of the furan heterocycle likely undergoes a mechanism involving anionic fullerene species. Notably, there are also some polar reaction products that cannot be eluted from the silica column. Further increase of I_2 to 6 equiv with respect to C_{60} (entry 5) resulted in a significant amount of methanofullerene (**3**) along with the monofuran adduct (**2**), demonstrating that the cyclopropanation of C_{60} is preferred in the presence of more I_2, and suggesting that cyclopropanation of C_{60} likely proceeds via a radical addition mechanism, as there would be fewer carbanions in the presence of more I_2. In addition, the reaction also results in bisadducts that are not well resolved and difficult to purify. These bisadducts are not bisdihydrofuran C_{60} derivatives, judging by the HPLC retention time, and they are likely related to the bismethanofullerenes as reported previously.[10] Further increase of OH^- and I_2 to 10 and 11 equiv with respect to C_{60} (entry 6) resulted in more polar products that are hardly eluted from the silica column, indicating it is not suitable for preparing bisdihydrofuran C_{60} derivatives. An increase of the reaction temperature to 80 °C (entry 7) is unfavorable for the reaction, where most products are insoluble in toluene.

Figure 2 displays the HPLC trace of the reaction mixture obtained under the conditions of entry 4 in Table 1, which shows four well resolved fractions labeled as **1a**, **1b**, **1c**, and **1d** corresponding to the bis-2′,3′-dihydrofurano[60]fullerene regioisomers and one fraction due to the mono-2′,3′-dihydrofurano[60]fullerene (**2**). The HRMS of **1a**, **1b**, **1c**, and **1d** (Figures S2, S8, S14, and S20) show protonated molecular ions at 977.09942, 977.09965, 977.09922, and 977.09929, respectively, which are well matched with those of the protonated bis-2′,3′-dihydrofurano[60]fullerene ($C_{72}H_{17}O_6^+$, calcd 977.10196), indicating they are all regioisomers of **1**.

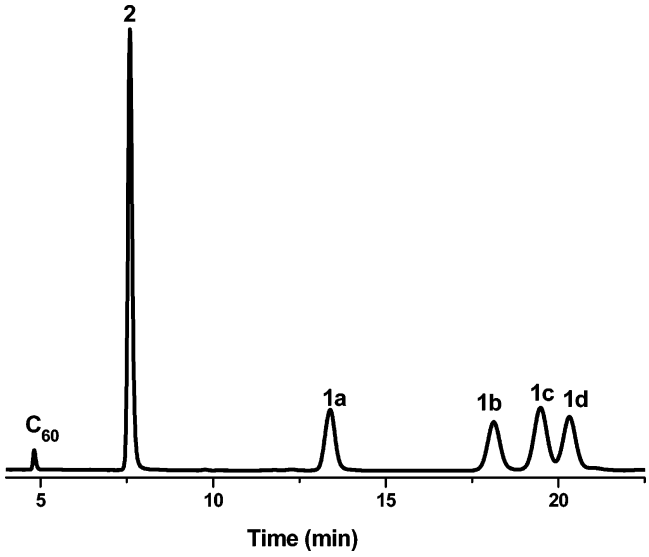

Figure 2. HPLC trace of the crude reaction mixture obtained from the reaction of [60]fullerene with OH^- and ethyl acetoacetate quenched with I_2. The mixture was eluted with a mixture of 3:2 *v*/*v* toluene/hexane over a silica column (10 × 250 mm) at a flow rate of 4 mL/min with the detector wavelength set at 380 nm.

The structural information for **1a**, **1b**, **1c**, and **1d** is first revealed by the HPLC elution order. Previous work on HPLC separation of C_{60} bisadducts over a silica or similar column has shown that these regioisomers are generally eluted in the sequence of *trans*-1, *trans*-2, *trans*-3, *trans*-4, *e*, *cis*-3, *cis*-2, and *cis*-1, in accordance with the increasing order of polarity for these derivatives, even though the elution order may slightly change in certain cases.[1c,2] The result indicates that fraction **1a**, the first fraction after the mono-2′,3′-dihydrofurano[60]-fullerene **2**, is likely the *trans*-1 bis-2′,3′-dihydrofurano[60]-fullerene, while the subsequent three fractions **1b**, **1c**, and **1d** may be related to the *trans*-2, *trans*-3, *trans*-4, or *e* regioisomers accordingly, as it is possible that the elution order may have a slight variation or that one of the configurations is not formed.

Figure 3 shows all the possible regioisomers of **1** with *trans*-1, *trans*-2, *trans*-3, *trans*-4, and *e* configurations along with the symmetry of each individual molecule. Different from C_{60} bisadducts with symmetrical addends, each *trans*-2, *trans*-3, and *trans*-4 fraction of **1** is composed of three possible regioisomers, while *trans*-1 and *e* fractions are composed of two possible regioisomers due to the unsymmetry nature of the addend. Computational calculations with Gaussian 09 at B3LYP/6-31G predicts that all the possible respective regioisomers are stable for the *trans*-1, *trans*-2, *trans*-3, *trans*-4, and *e* configurations, with only a small energy difference among them (Table S1).

The structural assignment of the four bis-dihydrofurano[60]-fullerenes is achieved by spectroscopic characterizations, where the UV−vis, ^1H NMR, and ^{13}C NMR spectra play a key role. Figure 4 and Figure 5 show the ^1H NMR and UV−vis spectra of **1a**, **1d**, **1c**, and **1b**, which are in the order of the structural determination as discussed below.

DOI: 10.1021/acs.joc.5b02392
J. Org. Chem. 2016, 81, 121−128

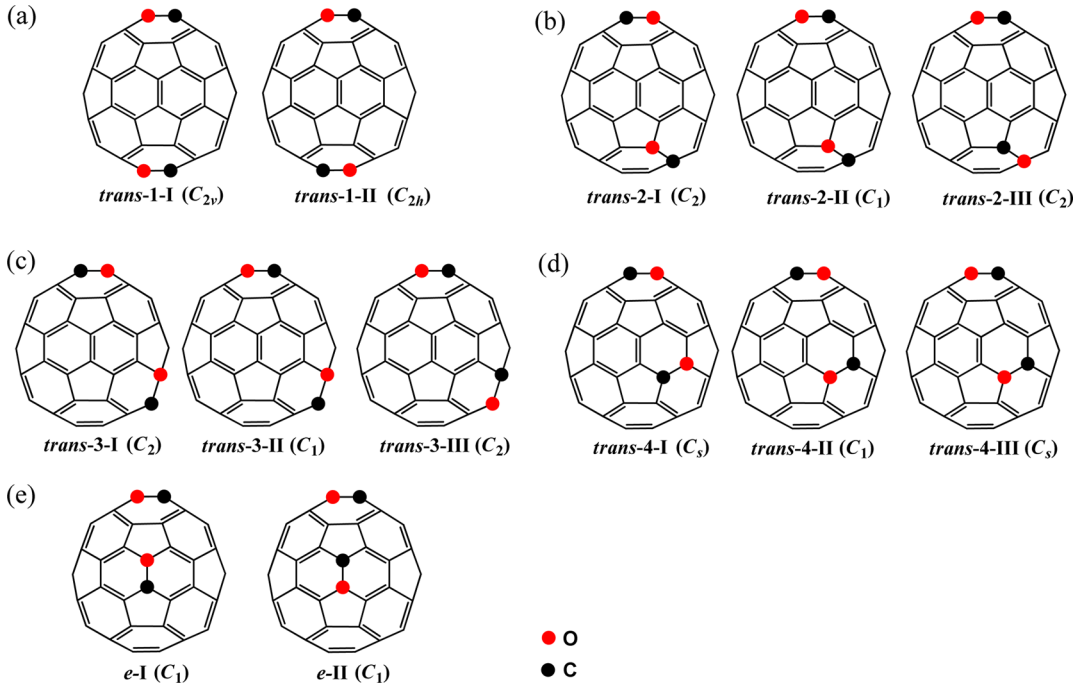

Figure 3. Structural illustrations of (a) *trans*-1, (b) *trans*-2, (c) *trans*-3, (d) *trans*-4, and (e) *e* adducts.

Structural Determination of 1a. The confirmation of **1a** as *trans*-1 adducts is achieved with the ^{1}H and ^{13}C NMR characterizations. Figure 4a displays the ^{1}H NMR spectrum of **1a**, which shows two sets of signals with different intensity for the 5′-methyl (2.778, 2.909 ppm) and acetate (1.383, 1.486 ppm; 4.438, 4.506 ppm). The ^{13}C and HMBC NMR spectra of **1a** (Figures S4−S6) also show two sets of signals with different intensity for the carbon atoms of methyl in the acetate and the 5′-methyl (14.35, 14.46 ppm; 15.42, 15.56 ppm), the methylene carbon in the acetate group (60.71, 60.79 ppm), the C_{60} carbon atoms bound to the carbon and oxygen atoms of the addends (71.42, 71.75 ppm; 101.98, 102.42 ppm), the 4′-carbon atom of the heterocycle (105.29, 105.65 ppm), the carbonyl carbon atom of the acetate (165.00, 165.10 ppm), and the 5′-carbon atom of the heterocycle (169.09, 169.32 ppm). More importantly, the signals corresponding to the sp^2 C_{60} carbon atoms can also be classified into two types, with a total of 28 peaks for the more intense signals, and 20 peaks for the less intense signals. The result indicates that fraction **1a** is composed of two regioisomers with at least C_2 or C_s symmetry. Among all the eight possible C_{60} bisadducts (*trans*-1, *trans*-2, *trans*-3, *trans*-4, *e*, *cis*-3, *cis*-2, and *cis*-1; Figure S35 for structural illustrations of the *cis*-1, *cis*-2 and *cis*-3 adducts),[1] only the *trans*-1 bis-2′,3′-dihydrofurano[60]fullerene can satisfy such a requirement by having two regioisomers with C_{2h} and C_{2v} symmetry as shown in Figure 3. In principle, the *trans*-1-I (C_{2v}) and the *trans*-1-II (C_{2h}) regioisomers are expected to exhibit 15 (13 × 4C + 2 × 2C) and 14 (14 × 4C) peaks for the sp^2 carbons of C_{60}, respectively. However, it is possible that symmetry of molecules may be reduced caused by the slow movement of the bulky addends at the ^{13}C NMR time scale, and subsequently more peaks could appear in the ^{13}C NMR spectra. The NMR characterization and HPLC elution order demonstrate unambiguously that fraction **1a** consists of the *trans*-1 bis-2′,3′-dihydrofuran C_{60} derivatives. The UV−vis spectrum of **1a** (Figure 5a) shows a strong broad absorption band at 476 nm and a weak absorption band at 701 nm, which is, in general, similar to those of the *trans*-1 regioisomers,[1c,2] consistent with the structural assignment.

Structural Determination of 1d. According to the HPLC elution order, fraction **1d** is likely associated with the *trans*-4 or *e* regioisomers. The composition of fraction **1d** is determined by the NMR and UV−vis characterizations. Figure 4b displays the ^{1}H NMR spectrum of **1d**, which shows two sets of signals for the 5′-methyl (2.662, 2.688 ppm) and acetate group (1.219, 1.375 ppm; 4.250, 4.365 ppm), similar to the situation of **1a**. However, different from that of **1a**, the two sets of signals have identical intensity, indicating that they are likely to originate from the two different hydrofuran heterocycles of the same molecule that has C_1 symmetry. The ^{13}C and HMBC NMR spectra of **1d** (Figures S22−S24) also exhibit two sets of signals with almost identical intensity for the carbon atoms of methyl in the acetate and the 5′-methyl (14.21, 14.30 ppm; 15.33, 15.40 ppm), the methylene carbon in the acetate group (60.42, 60.58 ppm), the C_{60} carbon atoms (70.97, 71.30 ppm; 101.23, 101.48 ppm) bound to the carbon and oxygen atoms of the addends, the 4′-carbon atom of the heterocycle (104.51, 104.74 ppm), the carbonyl carbon atom of the acetate (164.63, 164.72 ppm), and the 5′-carbon atom of the heterocycle (168.60, 169.18 ppm), consistent with the ^{1}H NMR result. In addition, a total of 49 signals, among which 43 have almost the same intensity, are shown for the sp^2 C_{60} carbon atoms. The result indicates that fraction **1d** is composed of only one regioisomer that has C_1 symmetry.

The UV−vis spectrum of **1d** (Figure 5b) shows a strong absorption band at 417 nm, which is the characteristic absorption for the *e* isomer,[1c,2] indicating explicitly that fraction **1d** is composed of the *e* regioisomer, consistent with the C_1 symmetry of *e* regioisomers. Even though computational calculations predict that both *e* regioisomers are thermodynamically stable (Table S1), the NMR characterization indicates that only one regioisomer is formed. Such a result suggests that one of the *e* regioisomers is likely unfavored during the formation process, where the steric factor may play a key role. An

DOI: 10.1021/acs.joc.5b02392
J. Org. Chem. 2016, 81, 121−128

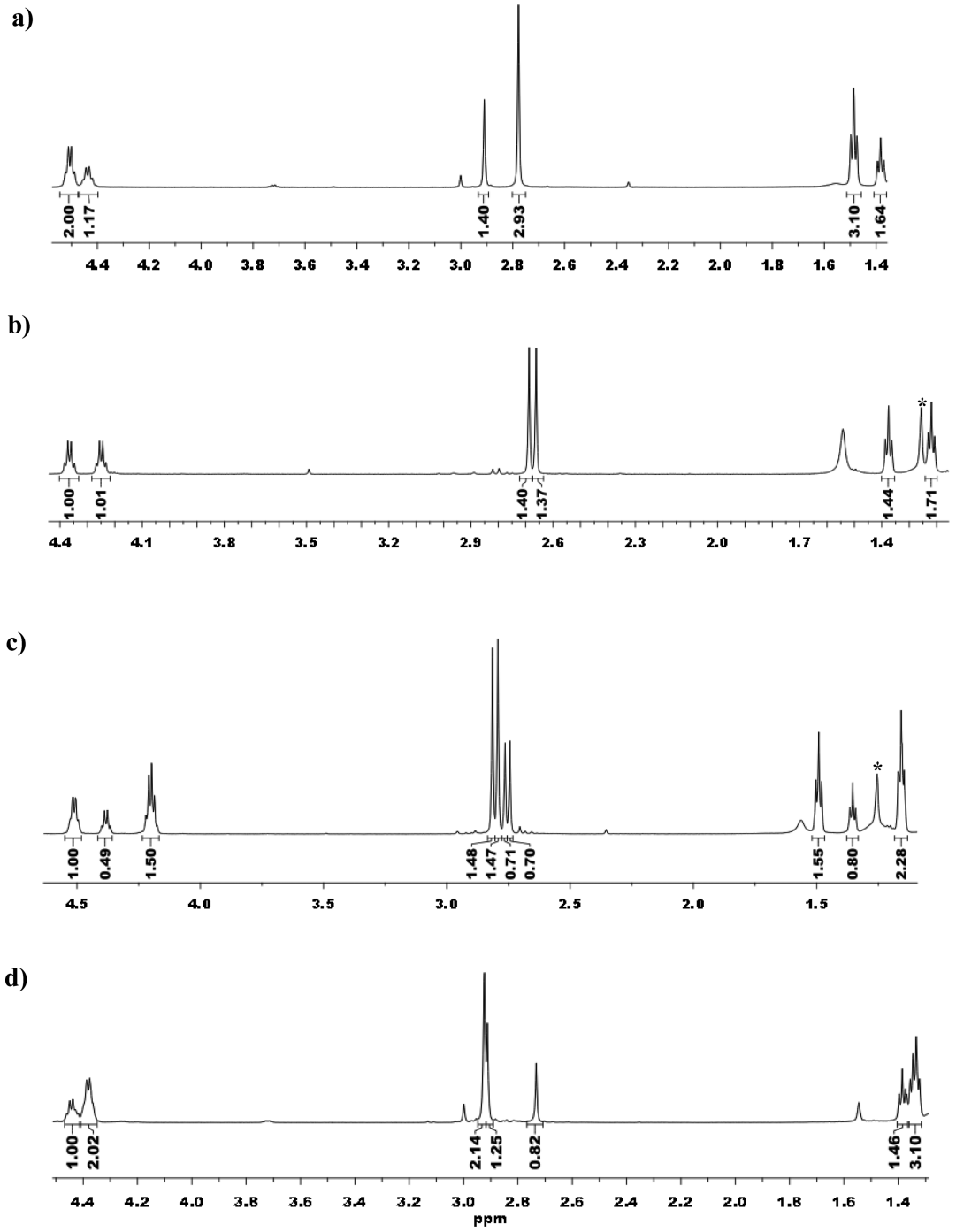

Figure 4. [1] H NMR (600 MHz) spectra of (a) **1a**, (b) **1d**, (c) **1c**, and (d) **1b** recorded in $CDCl_3$. The peak at 1.56 ppm is due to H_2O residue, and the peak labeled with an asterisk is due to an unknown impurity.

examination of the optimized *e*-II regioisomer (Figure S33) reveals that it has one of the acetates pointed toward a rigid furan ring, which may bring considerable steric hindrance during the formation of the second furan, caused by the C_{60}–C(acetate) bond rotation before ring closure (see Scheme 1 for the proposed reaction mechanism). The result therefore indicates that fraction **1d** is likely composed of the *e*-I regioisomer of **1**.

Structural Determination of 1c. With the assignment of **1a** and **1d** as the *trans*-1 and *e* regioisomers, it is rational to assume that fractions **1b** and **1c** are among the *trans*-2, *trans*-3, and *trans*-4 regioisomers according to the HPLC elution order. The structure of **1c** is resolved by the UV–vis spectroscopy. The spectrum of **1c** (Figure 5c) shows absorptions at 453, 488, 619, and 680 nm, which matches well with the absorptions of *trans*-3 regioisomers in previous work,[1c,2] indicating that fraction **1c** corresponds to the *trans*-3 adducts.

Further structural assignment of **1c** is achieved by the NMR characterizations. Figure 4c displays the ^{1}H NMR spectrum of **1c**. The spectrum shows four signals for the 5′-methyl (2.745, 2.764, 2.793, 2.815 ppm), which can be classified into two sets of signals. Three sets of signals with different intensities are shown for the acetates (1.158, 1.342, 1.492 ppm; 4.203, 4.365, 4.505 ppm), indicating the presence of three regioisomers in

DOI: 10.1021/acs.joc.5b02392
J. Org. Chem. 2016, 81, 121–128

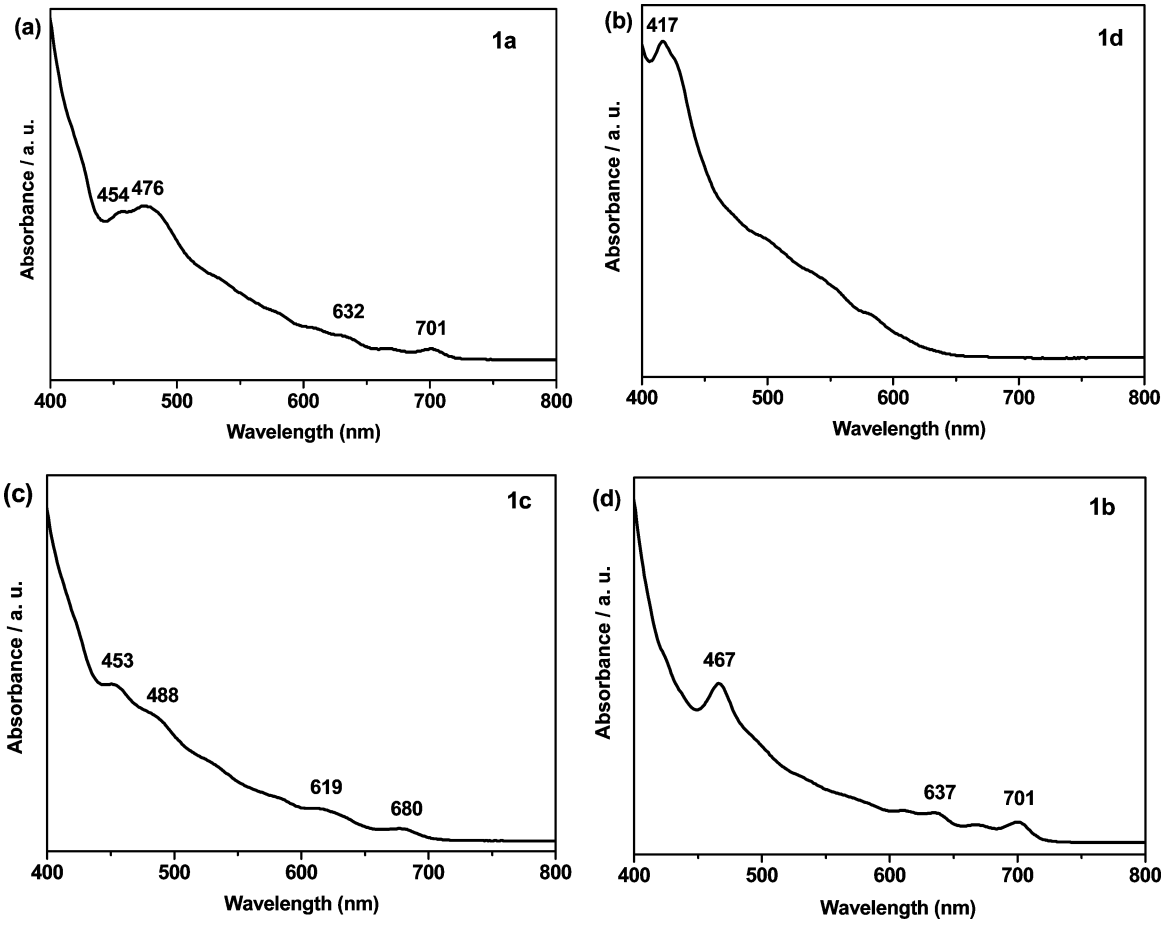

Figure 5. UV−vis spectra of (a) **1a**, (b) **1d**, (c) **1c**, and (d) **1b** recorded in toluene.

Scheme 1. Proposed Mechanism for the Formation of Regioisomeric 1

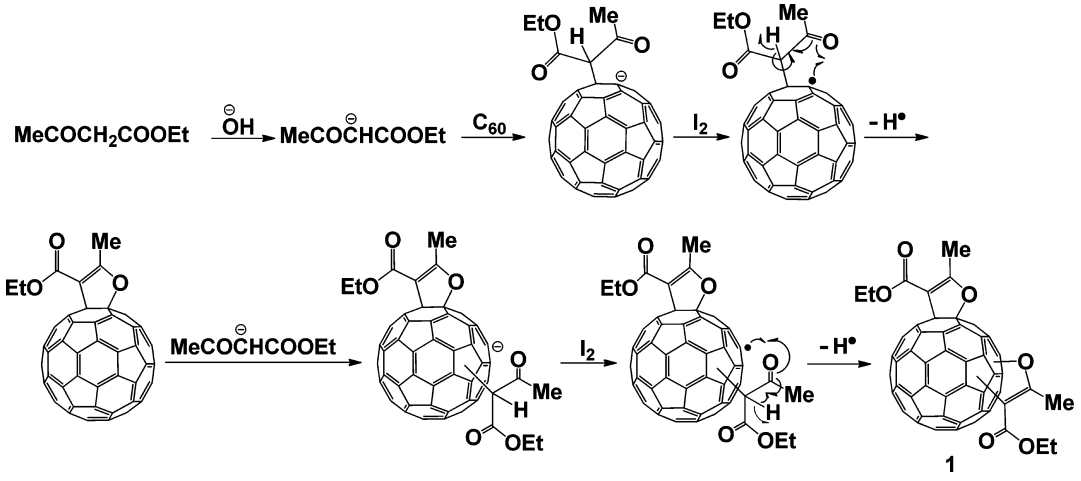

the fraction. The exhibition of two sets of signals for the 5′-methyl protons is likely due to the incidental overlapping of signals from two of the regioisomers. The appearance of the two closely positioned peaks with the same intensity within each set of signals suggests a symmetry reduction for the C_2 regioisomers likely caused by the slow movement of the bulky addends. The ^{13}C and HMBC NMR spectra of **1c** (Figures S16−S18) show three sets of signals with different intensity for the carbon atoms of methyl in the acetate and the 5′-methyl (14.12, 14.34, 14.47 ppm; 15.38, 15.42, 15.47 ppm), the methylene carbon atom in the acetate group (60.42, 60.62, 60.77 ppm), and four sets of signals for the C_{60} carbon atoms bound to the carbon and oxygen atoms of the addends (71.04, 71.32, 71.43, 71.78 ppm; 102.01, 102.44, 102.57, 102.70 ppm), the 4′-carbon atom of the heterocycle (104.64, 105.09, 105.23, 105.42 ppm), the carbonyl carbon atom of the acetate (164.61, 164.65, 164.94, 165.04 ppm), and the 5′-carbon atom of the heterocycle (168.99, 169.20, 169.39, 169.58 ppm). The appearance of four sets of peaks for certain carbons is likely due to the symmetry reduction of regioisomers as observed in

DOI: 10.1021/acs.joc.5b02392
J. Org. Chem. 2016, 81, 121−128

the ^{1}H NMR and agrees with the presence of three regioisomers in fraction **1c**. A total of 90 peaks corresponding to the sp^2 C_{60} carbon atoms are shown in the ^{13}C NMR spectrum of **1c**, consistent with the presence of 2 C_2 and 1 C_1 regioisomers.

Structural Determination of 1b. With the identification of **1a**, **1c**, and **1d** as the *trans*-1, *trans*-3, and *e* regioisomers, respectively, fraction **1b** is likely due to the *trans*-2 regioisomer rather than *trans*-4 adduct according to the HPLC elution order. The UV−vis spectrum of **1b** (Figure 5d) shows a major absorption band at 467 nm and weak absorption bands at 637 and 701 nm, which is essentially identical to the absorptions of the *trans*-2 regioisomers but very different from those of the *trans*-4 regioisomers,[1c,2] confirming that fraction **1b** consists of the *trans*-2 regioisomers.

Figure 4d displays the ^{1}H NMR spectra of **1b**, which shows three sets of signals with different intensity for the 5′-methyl (2.732, 2.912, 2.924 ppm) but two sets of signals for the acetates (1.333, 1.369 ppm; 4.380, 4.434 ppm), consistent with the presence of three regioisomers. The ^{13}C and HMBC NMR spectra of **1b** (Figures S10 and S12) show two sets of signals with different intensity for the carbon atoms of methyl in the acetate and the 5′-methyl (14.11, 14.32 ppm; 15.40, 15.54 ppm), the methylene carbon atom in the acetate group (60.64, 60.70 ppm), the C_{60} carbon atoms bound to the carbon atoms of the addends (71.18, 71.50 ppm), the carbonyl carbon atom of the acetate (164.91, 165.09 ppm), and four sets of signals for the C_{60} carbon atoms bound to the oxygen atoms of the addends (102.34, 102.49, 103.27, 103.37 ppm), the 4′-carbon atom of the heterocycle (105.68, 105.71, 106.07, 106.24 ppm), and the 5′-carbon atom of the heterocycle (169.25, 169.31, 169.35, 169.42 ppm). The appearance of two sets of resonances may be related to the incidental overlapping of peaks, while the exhibition of four peaks may be due to the symmetry reduction of individual regioisomer at the ^{13}C NMR time scale. Notably, a total of 98 peaks corresponding to the sp^2 C_{60} carbon atoms are shown in the ^{13}C NMR spectrum of **1b**, which further supports the presence of two C_2 regioisomers and one C_1 regioisomer in the fraction, consistent with the assignment of **1b** as the *trans*-2 regioisomers.

Steric Effect on the Regioselectivity and Mechanistic Consideration. Previous work has proposed that the regioselectivity of the C_{60} bisaddition is significantly affected by the frontier orbital distribution in the monoadduct, with the preferential formation of the *cis*-1, *e*, and *trans*-3 bisadducts when less sterically demanding addends are used.[1,2] The regioselectivity of the C_{60} bisaddition may also be affected by the steric factor introduced by the bulky addends, where the formation of the *cis*-1 regioisomer is severely inhibited as shown previously.[1,2] However, no work regarding whether such a steric factor may further suppress the formation of other *cis* regioisomers or enhance the formation of the *trans* regioisomers has been reported. Figure 6 displays the relative yields of the bis-2′,3′-dihydrofurano[60]fullerenes, which are calculated as 22:22:30:26 on the basis of the HPLC peak area ratio of **1a**, **1b**, **1c**, and **1d**. Relative yields for the Hirsch bisadducts[1b] and benzyne bisadducts[2b] of C_{60}, which have less sterically demanding addends, are also shown in the figure for comparison. Impressively, the formation of all *cis* regioisomers is inhibited for the case of bis-2′,3′-dihydrofurano[60]-fullerenes, but the formation of the *trans* adducts, especially the *trans*-1 adduct, an isomer that is otherwise difficult to be obtained when less bulky addends are used, is significantly

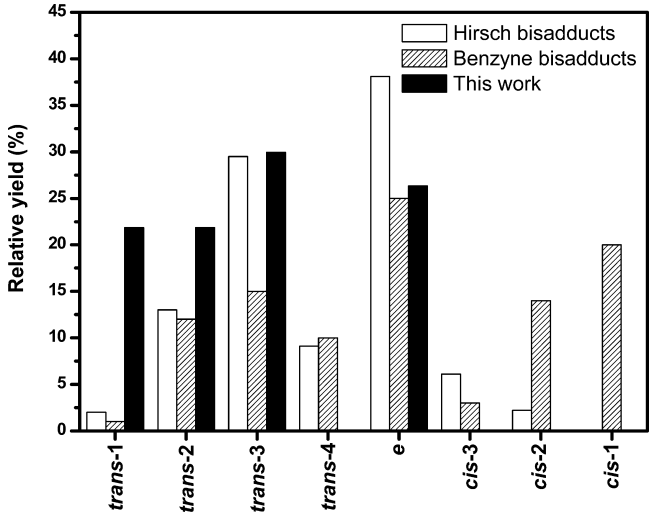

Figure 6. Relative yields for the formation of regioisomeric **1**, Hirsch bisadducts, and benzyne bisadducts. The values for Hirsch and benzyne bisadducts of C_{60} are taken from refs 1b and 2b, respectively.

enhanced, providing new insight into the steric effect on the regioselectivity of bisaddition to C_{60}. Even though the *trans*-4 regioisomers are predicted to be stable (Table S1), no *trans*-4 regioisomers are obtained from the reaction, likely due to the steric hindrance encountered during the formation process, as the bulky addends are expected to have the closest contact in the *trans*-4 adducts among all the *trans* regioisomers.

The LUMO distribution for **2** was calculated with Gaussian 09 at B3LYP/6-311G(d) level. The result shows a typical distribution for C_{60} monoadducts, where the LUMO is mainly localized at the *cis*-1, *e*, and *trans*-3 sites, with only a trivial amount at the *trans*-1 site (Figure S34). The result therefore demonstrates that it is the steric factor rather than any electronic factor that enhances the formation the *trans*-1 regioisomers of **1**.

A reaction mechanism for the formation of bis-2′,3′-dihydrofurano[60]fullerenes is proposed as shown in Scheme 1 on the basis of reaction screening and previous work for the synthesis of mono-2′,3′-dihydrofurano[60]fullerene.[6b] The reaction is initiated by the abstraction of α-hydrogen of ethyl acetoacetate to generate enolate anion intermediate, which would attack C_{60} via a nucleophilic addition pathway and gradually form the mono-2′,3′-dihydrofurano[60]fullerene (**2**) via oxidative cycloaddition by reaction with I_2. The addition of the second enolate anion intermediate is crucial in formation of **1**. It requires the use of excessive OH^- to generate extra enolate anion for the second-step addition. In the meanwhile, the amount of I_2 is crucial in accomplishing the reaction. In the presence of excessive I_2, the enolate anions may be oxidized into radicals before nucleophilic addition to C_{60}, which may result in the methanofullerene or related bisadducts.[10] When less I_2 is present, a large amount of anionic fullerene species may be produced in solution, which would result in more insoluble polymeric epoxide materials once the solution is exposed to ambient conditions during the following workup.[8,9]

■ CONCLUSION

The base-promoted oxidative cycloaddition reaction of C_{60} with ethyl acetoacetate is studied. The reaction has afforded C_{60} bisadducts bearing 2′,3′-dihydrofuran heterocycles for the first time. More importantly, the work demonstrates a completely

DOI: 10.1021/acs.joc.5b02392
J. Org. Chem. 2016, 81, 121−128

unprecedented effect of the steric factor on the regioselectivity of C_{60} bisaddition, where the formation of all the *cis* regioisomers is inhibited, while the formation of the *trans* regioisomers, especially the *trans*-1 regioisomer that is otherwise difficult to be obtained, is greatly enhanced, providing a new perspective on regiocontrol from steric influence. In addition, the product distribution in each specific configuration of bisadduct is complicated by the use of unsymmetrical addends, which has been studied with spectroscopic characterizations and computational calculations.

EXPERIMENTAL SECTION

General Methods. All reactions were carried out under an atmosphere of Ar. All reagents were obtained commercially and used without further purification.

Preparation of [60]Fullerene Bisadducts 1a–d. Typically, 36 mg of C_{60} and 500 μL of ethyl acetoacetate (79 equiv) were added to *o*-DCB (15 mL) and degassed with argon for 15 min with vigorous stirring at room temperature. Then 5 equiv of TBAOH (1.0 M in methanol, 250 μL) was added to the solution, and the reaction was allowed to proceed for 30 min. The reaction mixture was then quenched with 2.2 equiv of I_2 (27.5 mg) for 5 min, and the mixture was dried with a rotary evaporator under reduced pressure. The residue was washed with methanol to remove excess TBAOH and I_2. The crude product was first eluted with toluene over a flash silica gel column to remove any materials having strong polarity. The eluted mixture was then purified over a semipreparative silica column (10 mm × 250 mm), eluting with a mixture of toluene/hexane (*v*/*v*, 3:2) at a flow rate of 3.7 mL/min with the detector wavelength set at 380 nm. Compound **2** was obtained in a yield of 17% (7 mg), and a regioisomeric mixture of **1** was obtained in a yield of 27% (13 mg).

Spectral Characterization of 1a. Positive ESI FT-ICR MS, *m*/*z* calcd for $C_{72}H_{17}O_6^+$ $[M + H]^+$ 977.10196, found 977.09942; ^{1}H NMR (600 MHz, $CDCl_3$) δ 4.51 (q, J = 7.2 Hz), 4.44 (q, J = 7.2 Hz), 2.91 (s), 2.78 (s), 1.49 (t, J = 7.2 Hz), 1.38 (t, J = 7.2 Hz); ^{13}C NMR (150 MHz, $CDCl_3$) δ 169.32 ($OCCH_3$), 169.09 ($OCCH_3$), 165.10 (*C*═O), 165.00 (*C*═O), 150.15, 149.96, 149.70, 149.25, 149.18, 148.49, 148.30, 148.20, 147.00, 146.95, 146.85, 146.68, 146.43, 146.37, 146.12, 145.91, 145.88, 145.80, 145.67, 145.45, 145.36, 145.08, 144.87, 144.76, 144.45, 144.41, 144.12, 143.95, 143.70, 143.65, 143.33, 143.24, 143.10, 142.59, 142.49, 142.25, 142.06, 141.80, 141.15, 140.42, 139.81, 139.43, 139.25, 138.59, 137.52, 136.05, 135.51, 134.02, 105.65 (*CC*═O), 105.29 (*CC*═O), 102.42 (sp^3 C of C_{60}, C_{60}–O), 101.98 (sp^3 C of C_{60}, C_{60}–O), 71.75 (sp^3 C of C_{60}, C_{60}–C), 71.42 (sp^3 C of C_{60}, C_{60}–C), 60.79 (CH_2), 60.71 (CH_2), 15.56 (CH_3), 15.42 (CH_3), 14.46 (OCH_2CH_3), 14.35(OCH_2CH_3); UV–vis (400–800 nm, toluene) λ_{max}: 454, 476, 632, and 701 nm.

Spectral Characterization of 1b. Positive ESI FT-ICR MS, *m*/*z* calcd for $C_{72}H_{17}O_6^+$ $[M + H]^+$ 977.10196, found 977.09965; ^{1}H NMR (600 MHz, $CDCl_3$) δ 4.46–4.42 (m), 4.39–4.37 (m), 2.92(s), 2.91 (s), 2.73(s), 1.40–1.37 (m), 1.36–1.32(m); ^{13}C NMR (150 MHz, $CDCl_3$) δ 169.42 ($OCCH_3$), 169.35 ($OCCH_3$), 169.31 ($OCCH_3$), 169.25 ($OCCH_3$), 165.09 (*C*═O), 164.91 (*C*═O), 151.50, 151.32, 150.50, 150.27, 150.24, 150.17, 149.87, 149.76, 149.41, 149.27, 149.21, 149.00, 148.53, 148.03, 147.95, 147.86, 147.82, 147.59, 147.55, 147.50, 147.30, 147.20, 146.97, 146.93, 146.85, 146.74, 146.62, 146.57, 146.51, 146.49, 146.44, 146.37, 146.33, 146.14, 146.11, 145.85, 145.82, 145.75, 145.72, 145.65, 145.59, 145.50, 145.20, 144.97, 144.92, 144.77, 144.74, 144.52, 144.41, 144.34, 144.24, 144.15, 144.07, 144.03, 143.86, 143.49, 143.40, 143.30, 143.17, 143.09, 143.01, 142.97, 142.74, 142.66, 142.57, 142.49, 142.31, 142.14, 142.11, 141.88, 141.77, 141.67, 141.60, 141.55, 141.41, 141.10, 140.87, 140.83, 140.77, 140.54, 139.98, 139.75, 139.64, 139.55, 139.34, 138.99, 137.77, 137.74, 137.40, 136.67, 136.11, 135.93, 135.87, 134.84, 134.58, 133.64, 133.18, 132.78, 106.24 (*CC*═O), 106.07 (*CC*═O), 105.71 (*CC*═O), 105.68 (*CC*═O), 103.37 (sp^3 C of C_{60}, C_{60}–O), 103.27 (sp^3 C of C_{60}, C_{60}–O), 102.49 (sp^3 C of C_{60}, C_{60}–O), 102.34 (sp^3 C of C_{60}, C_{60}–O), 71.50 (sp^3 C of C_{60}, C_{60}–C), 71.18 (sp^3 C of C_{60}, C_{60}–C), 60.70 (CH_2), 60.64 (CH_2), 15.54 (CH_3), 15.40 (CH_3), 14.32 (OCH_2CH_3), 14.11 (OCH_2CH_3); UV–vis (400–800 nm, toluene) λ_{max}: 467, 637, and 701 nm.

Spectral Characterization of 1c. Positive ESI FT-ICR MS, *m*/*z* calcd for $C_{72}H_{17}O_6^+$ $[M + H]^+$ 977.10196, found 977.09922; ^{1}H NMR (600 MHz, $CDCl_3$) δ 4.53–4.50 (m), 4.38 (q, J = 7.2 Hz), 4.22–4.18 (m), 2.82 (s), 2.79(s), 2.76 (s), 2.75 (s), 1.49 (t, J = 7.2 Hz), 1.35 (t, J = 7.2 Hz), 1.17–1.15 (m); ^{13}C NMR (150 MHz, $CDCl_3$) δ 169.58 ($OCCH_3$), 169.39 ($OCCH_3$), 169.20 ($OCCH_3$), 168.99 ($OCCH_3$), 165.04 (*C*═O), 164.94 (*C*═O), 164.65 (*C*═O), 164.61 (*C*═O), 151.04, 150.99, 150.63, 150.56, 150.16, 149.81, 149.71, 149.60, 149.44, 149.41, 149.30, 149.26, 149.18, 149.11, 148.94, 148.86, 148.80, 148.73, 148.60, 148.53, 148.25, 148.21, 147.68, 147.53, 147.21, 146.98, 146.93, 146.85, 146.63, 146.51, 146.42, 146.36, 146.15, 146.09, 146.02, 145.91, 145.79, 145.68, 145.54, 145.35, 145.31, 144.95, 144.91, 144.84, 144.72, 144.52, 144.42, 144.34, 144.27, 144.20, 143.81, 143.67, 143.59, 143.53, 143.27, 143.18, 143.04, 142.65, 142.54, 142.44, 142.33, 142.30, 142.24, 142.20, 141.98, 141.92, 141.86, 141.81, 141.61, 141.57, 141.49, 141.28, 140.50, 140.44, 140.02, 139.93, 139.17, 138.77, 138.27, 138.09, 137.96, 137.70, 137.25, 136.47, 136.02, 135.56, 135.37, 135.05, 132.84, 130.41, 105.42 (*CC*═O), 105.23 (*CC*═O), 105.09 (*CC*═O), 104.64 (*CC*═O), 102.70 (sp^3 C of C_{60}, C_{60}–O), 102.57 (sp^3 C of C_{60}, C_{60}–O), 102.44 (sp^3 C of C_{60}, C_{60}–O), 102.01 (sp^3 C of C_{60}, C_{60}–O), 71.78 (sp^3 C of C_{60}, C_{60}–C), 71.43 (sp^3 C of C_{60}, C_{60}–C), 71.32 (sp^3 C of C_{60}, C_{60}–C), 71.04 (sp^3 C of C_{60}, C_{60}–C), 60.77 (CH), 60.62 (CH), 60.42 (CH_2), 15.47 (CH_3), 15.42 (CH_3), 15.38 (CH_3), 14.47 (OCH_2CH_3), 14.34 (OCH_2CH_3), 14.12 (OCH_2CH_3); UV–vis (400–800 nm, toluene) λ_{max}: 453, 488, 619, and 680 nm.

Spectral Characterization of 1d. Positive ESI FT-ICR MS, *m*/*z* calcd for $C_{72}H_{17}O_6^+$ $[M + H]^+$ 977.10196, found 977.09929; ^{1}H NMR (600 MHz, $CDCl_3$) δ 4.37 (q, J = 7.2 Hz, 2H), 4.25 (q, J = 7.2 Hz, 2H), 2.69 (s, 3H), 2.66 (s, 3H), 1.38 (t, J = 7.2 Hz, 3H), 1.22 (t, J = 7.2 Hz, 3H); ^{13}C NMR (150 MHz, $CDCl_3$) δ 169.18 (1C, $OCCH_3$), 168.60 (1C, $OCCH_3$), 164.72 (1C, *C*═O), 164.63 (1C, *C*═O), 153.33(1C), 152.89(1C), 149.86(1C), 149.66(1C), 149.04(1C), 148.69(1C), 148.59(1C), 148.49(1C), 148.31(1C), 148.22(2C), 147.78(1C), 147.63(1C), 147.61(1C), 147.49(1C), 147.39(1C), 146.92(1C), 146.84(1C), 146.21(1C), 146.00(1C), 145.92(1C), 145.52(1C), 145.38(1C), 145.18(1C), 145.12(1C), 144.99(1C), 144.90(2C), 144.75(1C), 144.51(1C), 144.39(1C), 143.84(3C), 143.71(1C), 143.18(1C), 143.12(1C), 143.00(2C), 142.93(1C), 142.67(1C), 142.01(1C), 141.83(2C), 141.68(1C), 141.46(1C), 140.96(2C), 140.86(1C), 139.67(1C), 139.36(1C), 138.04(1C), 137.31(1C), 136.19(1C), 135.91(1C), 135.07(1C), 104.74 (1C, *CC*═O), 104.51 (1C, *CC*═O), 101.48 (1C, sp^3 C of C_{60}, C_{60}–O), 101.23 (1C, sp^3 C of C_{60}, C_{60}–O), 71.30 (1C, sp^3 C of C_{60}, C_{60}–C), 70.97 (1C, sp^3 C of C_{60}, C_{60}–C), 60.58 (1C, CH_2), 60.42 (1C, CH_2), 15.40 (1C, CH_3), 15.33 (1C, CH_3), 14.30 (1C, OCH_2CH_3), 14.21(1C, OCH_2CH_3); UV–vis (400–800 nm, toluene) λ_{max}: 417 nm.

Computational Methods. All calculations were performed with the Gaussian 09 software package using DFT/B3LYP. Geometry optimizations, harmonic vibrational frequencies, and the energy calculations were carried out at the B3LYP/6-31G level of theory.

ASSOCIATED CONTENT

Supporting Information

The Supporting Information is available free of charge on the ACS Publications website at DOI: 10.1021/acs.joc.5b02392.

HPLC traces, spectra of the new compounds, and calculation details (PDF)

AUTHOR INFORMATION

Corresponding Author

*E-mail: xgao@ciac.ac.cn.

Notes

The authors declare no competing financial interest.

DOI: 10.1021/acs.joc.5b02392
J. Org. Chem. 2016, 81, 121–128

■ ACKNOWLEDGMENTS

This work was supported by the National Natural Science Foundation of China, 21172212, 21202157, and 21472183.

■ REFERENCES

(1) (a) Hirsch, A.; Lamparth, I.; Grösser, T.; Karfunkel, H. R. *J. Am. Chem. Soc.* **1994**, *116*, 9385−9386. (b) Hirsch, A.; Lamparth, I.; Karfunkel, H. R. *Angew. Chem., Int. Ed. Engl.* **1994**, *33*, 437−438. (c) Djojo, F.; Herzog, A.; Lamparth, I.; Hampel, F.; Hirsch, A. *Chem. - Eur. J.* **1996**, *2*, 1537−1547.

(2) (a) Nakamura, Y.; O-kawa, K.; Matsumoto, M.; Nishimura, J. *Tetrahedron* **2000**, *56*, 5429−5434. (b) Nakamura, Y.; Takano, N.; Nishimura, T.; Yashima, E.; Sato, M.; Kudo, T.; Nishimura, J. *Org. Lett.* **2001**, *3*, 1193−1196. (c) Kordatos, K.; Bosi, S.; Da Ros, T.; Zambon, A.; Lucchini, V.; Prato, M. *J. Org. Chem.* **2001**, *66*, 2802−2808.

(3) (a) Lenes, M.; Wetzelaer, G.-J. A. H.; Kooistra, F. B.; Veenstra, S. C.; Hummelen, J. C.; Blom, P. W. M. *Adv. Mater.* **2008**, *20*, 2116−2119. (b) He, Y.; Chen, H.-Y.; Hou, J.; Li, Y. *J. Am. Chem. Soc.* **2010**, *132*, 1377−1382. (c) Meng, X.; Zhang, W.; Tan, Z.; Du, C.; Li, C.; Bo, Z.; Li, Y.; Yang, X.; Zhen, M.; Jiang, F.; Zheng, J.; Wang, T.; Jiang, L.; Shu, C.; Wang, C. *Chem. Commun.* **2012**, *48*, 425−427.

(4) (a) Li, C.-Z.; Yip, H.-L.; Jen, A. K.-Y. *J. Mater. Chem.* **2012**, *22*, 4161−4177. (b) Li, Y. *Chem. - Asian J.* **2013**, *8*, 2316−2328.

(5) Ohno, M.; Yashiro, A.; Eguchi, S. *Chem. Commun.* **1996**, 291−292.

(6) (a) Wang, G.-W.; Zhang, T.-H.; Li, Y.-J.; Lu, P.; Zhan, H.; Liu, Y.-C.; Murata, Y.; Komatsu, K. *Tetrahedron Lett.* **2003**, *44*, 4407−4409. (b) Zhang, T.-H.; Wang, G.-W.; Lu, P.; Li, Y.-J.; Peng, R.-F.; Liu, Y.-C.; Murata, Y.; Komatsu, K. *Org. Biomol. Chem.* **2004**, *2*, 1698−1702. (c) Li, C.; Zhang, D.; Zhang, X.; Wu, S.; Gao, X. *Org. Biomol. Chem.* **2004**, *2*, 3464−3469. (d) Wang, G.-W.; Li, F.-B. *Org. Biomol. Chem.* **2005**, *3*, 794−797. (e) Li, F.-B.; Zhu, S.-E.; You, X.; Wang, G.-W. *Chin. Sci. Bull.* **2012**, *57*, 2269−2272.

(7) Hou, H.-L.; Li, Z.-J.; Sun, T.; Gao, X. *J. Org. Chem.* **2015**, *80*, 5315−5319 and references therein..

(8) (a) Winkler, K.; Costa, D. A.; Balch, A. L.; Fawcett, W. R. *J. Phys. Chem.* **1995**, *99*, 17431−17436. (b) Krinichnaya, E. P.; Moravsky, A. P.; Efimov, O.; Sobczak, J. W.; Winkler, K.; Kutner, W.; Balch, A. L. *J. Mater. Chem.* **2005**, *15*, 1468−1476.

(9) Hou, H.-L.; Gao, X. *J. Org. Chem.* **2012**, *77*, 2553−2558.

(10) Nierengarten, J.-F.; Felder, D.; Nicoud, J.-F. *Tetrahedron Lett.* **1998**, *39*, 2747−2750.

DOI: 10.1021/acs.joc.5b02392
J. Org. Chem. 2016, 81, 121−128